

# A Photochromic Histidine Kinase Rhodopsin (HKR1) That Is Bimodally Switched by Ultraviolet and Blue Light<sup>\*§</sup>

Received for publication, July 17, 2012, and in revised form, September 18, 2012. Published, JBC Papers in Press, October 1, 2012, DOI 10.1074/jbc.M112401604

Meike Luck<sup>†1</sup>, Tilo Mathes<sup>‡§2</sup>, Sara Bruun<sup>‡¶1</sup>, Roman Fudim<sup>‡1</sup>, Rolf Hagedorn<sup>‡</sup>, Tra My Tran Nguyen<sup>‡</sup>, Suneel Kateriya<sup>||</sup>, John T. M. Kennis<sup>§3</sup>, Peter Hildebrandt<sup>†</sup>, and Peter Hegemann<sup>‡4</sup>

From the <sup>†</sup>Institute of Biology, Experimental Biophysics, Humboldt-Universität zu Berlin, 10115 Berlin, Germany, the <sup>‡</sup>Faculty of Sciences, Department of Physics and Astronomy, Biophysics Group, Vrije Universiteit, De Boelelaan 1081, 1081 HV, Amsterdam, The Netherlands, the <sup>¶</sup>Institute of Chemistry, Technische Universität zu Berlin, Sekretariat PC14, Strasse des 17 Juni 135, 10623 Berlin, Germany, and the <sup>||</sup>Department of Biochemistry, University of Delhi South Campus, Benito Juarez Road, New Delhi, 110021, India

**Background:** Microbial rhodopsins in *Chlamydomonas* are employed for photoorientation and developmental processes.

**Results:** HKR1 is a UVA-absorbing rhodopsin that is bimodally switched between a UV- and a blue light-absorbing isoform with different light colors.

**Conclusion:** The chromophore of the dark-adapted UV state contains a deprotonated Schiff base stabilized by a 13-*cis*,15-*anti* conformation.

**Significance:** This is the initial characterization of the first member of a novel rhodopsin family.

Rhodopsins are light-activated chromoproteins that mediate signaling processes via transducer proteins or promote active or passive ion transport as ion pumps or directly light-activated channels. Here, we provide spectroscopic characterization of a rhodopsin from the *Chlamydomonas* eyespot. It belongs to a recently discovered but so far uncharacterized family of histidine kinase rhodopsins (HKRs). These are modular proteins consisting of rhodopsin, a histidine kinase, a response regulator, and in some cases an effector domain such as an adenylyl or guanylyl cyclase, all encoded in a single protein as a two-component system. The recombinant rhodopsin fragment, Rh, of HKR1 is a UVA receptor ( $\lambda_{\text{max}} = 380$  nm) that is photoconverted by UV light into a stable blue light-absorbing meta state Rh-Bl ( $\lambda_{\text{max}} = 490$  nm). Rh-Bl is converted back to Rh-UVA by blue light. Raman spectroscopy revealed that the Rh-UVA chromophore is in an unusual 13-*cis*,15-*anti* configuration, which explains why the chromophore is deprotonated. The excited state lifetime of Rh-UVA is exceptionally stable, probably caused by a relatively unpolar retinal binding pocket, converting into the photo-product within about 100 ps, whereas the blue form reacts 100 times faster. We propose that the photochromic HKR1 plays a role in the adaptation of behavioral responses in the presence of UVA light.

The main sensory photoreceptor of the animal kingdom is rhodopsin. The respective spectral sensitivity of rhodopsins

may cover an extremely broad range of the sunlight spectrum, from 358 nm (near ultraviolet, UVA) to 630 nm (near infrared) (1, 2). Rhodopsins with absorption at the red edge of the spectrum (XL-iodopsins) are found in flies, mollusks, fish, and in some birds. At this spectral range, thermal isomerization increases, producing significant background at high rhodopsin concentrations (3). On the other end of the spectrum, the UVA-absorbing pigment is of limited use because UV-transparent lenses promote damage of the retina. Even so, UV-sensitive rhodopsins are widely distributed in flies, birds, and nocturnal rodents (4, 5). Action and absorption spectra have been recorded for rhodopsins at both edges of the visible spectrum, but further spectroscopic studies based on the structure and dynamics of the photoreceptors are missing because of difficulties in purifying these proteins in sufficient amounts. In prokaryotes like archaea or eubacteria, rhodopsins serve as light-driven H<sup>+</sup> or Cl<sup>-</sup> pumps or mediate signal transduction via a two-component signaling system (6). Another branch that is rich in rhodopsin-related proteins is freshwater algae. Phototaxis of motile species like *Chlamydomonas reinhardtii* is mainly mediated by the light-gated ion channel channelrhodopsin, which is currently widely used in the new field of optogenetics to activate individual cells or cell types in brain slices or live animals to understand neuronal networks (7). Recently, a previously undescribed class of rhodopsin sequences has been found in several algal genomes including *C. reinhardtii* (8). These rhodopsins are directly connected via the C terminus to a histidine kinase and a response regulator, defining a novel rhodopsin subfamily of histidine-kinase rhodopsins (HKRs).<sup>5</sup> *C. reinhardtii* contains four HKR sequences, two of them with an additional cyclase domain (Fig. 1, A and B). They are believed to constitute functional two-component systems. It has been suggested that these HKRs are involved in cell cycle regulation

\* This work was supported by Deutsche Forschungsgemeinschaft Grants FOR1261 (to P. Hegemann), HE3824/19-1 (to S. B. and P. Hildebrandt), and Cluster of Excellence Grant UniCat/BIG-NSE.

† This article contains supplemental Figs. 1 and 2.

<sup>‡</sup> Supported by the LaserLab Europe access program LCVU001753.

<sup>§</sup> Supported by the Chemical Sciences Council of The Netherlands Organization for Scientific Research through an ECHO grant (to J. T. M. K.). Supported by NWO-DFG Bilateral program.

<sup>¶</sup> Supported by a Chemical Sciences Council of The Netherlands Organization for Scientific Research VIDI grant. Supported by NWO-DFG Bilateral program.

<sup>||</sup> Supported by NWO-DFG Bilateral program. To whom correspondence should be addressed. Tel.: 49-30-2093-8681; Fax: 49-30-2093-8520; E-mail: hegemann@rz.hu-berlin.de.

<sup>5</sup> The abbreviations used are: HKR, histidine kinase rhodopsin; Bl, blue; BR, bacteriorhodopsin; EADS, evolution-associated difference spectra; ESA, excited state absorption; GSB, ground state bleaching; LED, light-emitting diode; Rh, rhodopsin; RR, response regulator.

# A UV-sensitive Algal Rhodopsin

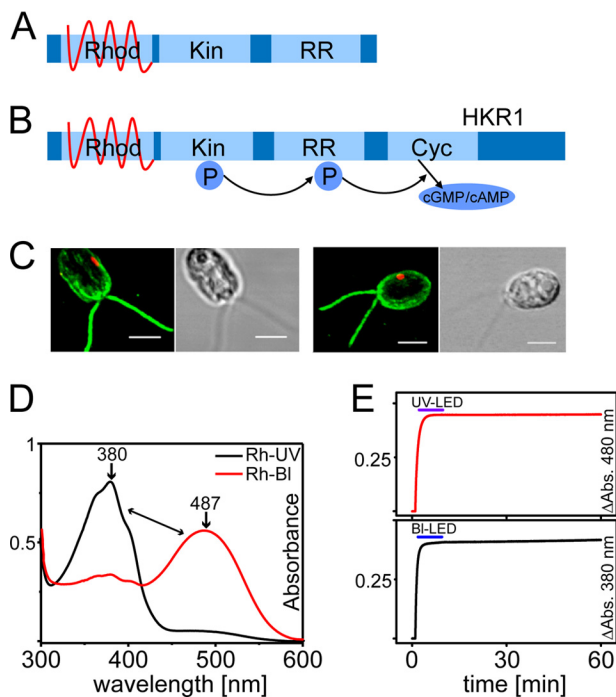


**FIGURE 1. Basic features of HKR1.** *A*, general modular assembly of HKRs. *B*, specific modular composition of HKR1 and HKR2 of *C. reinhardtii* (Rhod, rhodopsin; Kin, histidine kinase; RR, response regulator; Cyc, cyclase). *C*, localization of HKR1 in the *Chlamydomonas* eye using antibodies against Rh (red) in comparison with Nomarski images (left two panels) and against the response regulator RR (red; right two panels) combined with an  $\alpha$ -tubulin labeling (green). Scale bars, 4  $\mu$ m. *D*, absorption spectra of recombinant Rh-UV and Rh-Bl. *E*, stability of Rh-Bl (red line) and Rh-UV (black line). Absorbance changes were recorded during 10-min illumination and 50 min in darkness.

and circadian rhythmicity in the marine microalga *Ostreococcus*, but molecular characterization is still lacking (9).

## EXPERIMENTAL PROCEDURES

**Antibody Production and Immunolocalization**—Response regulator fragments of HKR1 (accession number AAQ16277) fused with a Sumo tag were expressed in *Escherichia coli* and purified under nondenaturing conditions by immobilized metal ion affinity chromatography. Approximately 3 mg of affinity-purified HKR1-RR protein was provided to a commercial facility (Genie, Bangalore, India) for raising polyclonal antibody in rabbit. The antigenicity of a peptide from the rhodopsin domain of HKR1 was predicted by the web-based Kolaskar and Tongaonkar antigenic prediction tool (10). The peptide was synthesized, and keyhole limpet hemocyanin was conjugated to its C terminus before injecting into rabbit. The specificity of each antibody was checked by immunoblotting by standard procedures using the respective affinity-purified proteins as antigens. Immunolocalization of HKR1 in *C. reinhardtii* was performed as described in the supplemental material.

**Protein Purification**—A humanized HKR1 sequence (amino acids 1–250) was heterologously expressed in the methylotrophic yeast *Pichia pastoris*. Protein production was induced by the addition of 2.5% methanol and 5  $\mu$ M all-*trans*-retinal to the growth medium. Protein purification was performed in a manner analogous to earlier described purification processes (11, 12) with modifications (see supplemental material). All spectroscopic studies were performed in a HEPES buffer, pH

7.4, containing 0.03% dodecyl maltoside. The pH dependence was tested using HEPES for pH 7.4 and 9 and citrate for pH 4.5 and 6.

**UV-Visible Absorption Spectroscopy and Flash Photolysis**—Absorption spectra and slow kinetics were recorded at 20 °C using a Cary 50 Bio spectrophotometer (Varian, Inc., Darmstadt, Germany) at a spectral resolution of 1.6 nm. Dark samples were measured after a dark adaptation period of 10 min. Light spectra were detected after a 1-min illumination with a 0.11-W UV-light-emitting diode (LED) (380 nm) or a 0.12-W blue LED (470 nm, both Nichia Corporation, Tokushima, Japan), respectively.

Transient spectroscopy was performed at 19 °C on an LKS.60 flash photolysis system (Applied Photophysics Ltd., Leatherhead, UK) equipped with a tunable Rainbow OPO/Nd:YAG laser system and an Andor iStar ICCD Camera with 2-nm resolution (Andor Technology, Belfast, Northern Ireland). Laser energy was adjusted to 3 millijoules/shot, and the pulse duration was 10 ns. When excited with 483- or 355-nm laser pulses, the samples were preilluminated for 2 s with four 375- or 470-nm LEDs (4  $\times$  0.1 W; Nichia Corporation, Tokushima, Japan), respectively. Further details have been described earlier (13, 14). For data analysis, we used MATLAB (Release 2012a; The MathWorks, Natick, MA) and identified the significant components of the system by singular value decomposition. Subsequent target analysis with a sequential kinetic model yielded the kinetic constants, the component spectra, and the reconstructed data set.

**Ultrafast Transient Spectroscopy**—Spectrally resolved femtosecond transient absorption spectroscopy with an instrument response function of 80 fs was carried out with a setup described earlier (15). To prevent multiple excitations of the same sample volume, the sample was moved in a Lissajous scanner as described previously (16). Data analysis was carried out with the Glotaran software package (17).

**Resonance Raman Spectroscopy**—Rh-UV/Bl. HKR1 (500  $\mu$ L;  $A_{380} \sim 3$ ) in H<sub>2</sub>O and D<sub>2</sub>O buffers (100 mM NaCl, 20 mM HEPES, 0.03% dodecyl maltoside, pH/pD 7.4) was measured using a LabRam confocal setup (18). Samples were continuously mixed, facilitated by a magnetic ball inside a rotating cuvette, and the accumulation time was 1 h at 1-mW excitation light. For Rh-Bl, the excitation wavelength was 514 nm and a background of UV LEDs (375 nm) was needed to accumulate sufficient amounts of this state. Without UV LED, Rh-Bl was excited by the laser to Rh-UV, and the spectra afforded only the Raman bands of the buffer. The spectra with and without UV LED were subtracted from each other to obtain the spectra free of buffer contributions. A similar procedure was used for the Rh-UV state, except for choosing an excitation line at 413 nm and blue LEDs (480 nm). Spectra were calibrated using toluene standard spectra, and a polynomial background was subtracted (BR-M410). Purified purple membrane from *H. halobium* strain S9 (2 mL,  $A_{570} \sim 2$ ; 10 mM Tris, pH 8) was measured using a 250-mW 514-nm pump and 25-mW 413-nm probe beams (delay time  $\sim$ 1 ms and spectra acquisition time  $\sim$ 4 h) using the rotating cuvette technique as described previously (19). The 413-nm probe-only spectrum was used to subtract the Raman

bands of the buffer. HPLC analysis of the extracted isomers of retinal was performed as described by Landers *et al.* (20).

## RESULTS

**Localization of HKR1 in the Eyespot of *Chlamydomonas***—As a first action we produced antisera against the rhodopsin fragment (Rh) and the response regulator portion (RR) of HKR1 to localize the protein in the alga. Both antisera identified a 170-kDa protein in the membrane fraction of *C. reinhardtii*. Both antisera allowed us to localize HKR1 within the eyespot area of the alga as seen in Fig. 1C.

**UV-Visible Spectroscopic Characterization of Heterologously Expressed HKR1-Rhodopsin**—In a second approach, we expressed the Rh fragment of HKR1 in the methylotrophic yeast *P. pastoris* complemented with all-*trans* retinal. The recombinant protein showed an absorption maximum at 380 nm (Fig. 1D), only a few nm shifted relative to the absorption of free retinal. However, the absorption was fine-structured, suggesting that the retinal was bound to protein without forming a protonated retinal Schiff base (12). Illumination of the protein with a 380-nm UV LED shifted the spectrum to 480 nm on the time scale of a few seconds (Fig. 1D). This blue-absorbing rhodopsin (Rh-Bl) was stable for hours (Fig. 1E), but it photochemically back-converted upon illumination with a blue LED (480 nm). Whereas the absorption spectra of Rh-UV and Rh-Bl were found to be pH-independent over the pH range from 6 to 9, we observed for Rh-UV an altered fine structure and a shift of the maximum of 5 nm for Rh-Bl at pH 4.5 (supplemental Fig. 1A).

**Chromophore Isomer Composition in HKR1**—To decipher retinal composition, we extracted in preliminary experiments the retinoids after reaction with hydroxylamine and separated the isomers by high pressure liquid chromatography (HPLC). Unexpectedly, 13-*cis* retinal was the dominant isomer in Rh-UV. In contrast, Rh-Bl showed an enhanced all-*trans* fraction, suggesting that at least the main photochemical reaction in going from Rh-UV to Rh-Bl is a 13-*cis* to all-*trans* isomerization. During the extraction procedure retinoids tend to thermally isomerize in favor of all-*trans*; therefore, we more thoroughly characterized the structures of the chromophores in Rh-UV and Rh-Bl using resonance Raman spectroscopy.

Resonance Raman spectra of the Rh-UV and Rh-Bl states of HKR1 were measured using 413-nm and 514-nm excitation, respectively. Photoconversion of Rh-UV and Rh-Bl by the exciting laser beam was compensated by continuous illumination with blue and UV LED light, respectively. The resonance Raman spectrum of Rh-Bl indicates the coexistence of two retinal isomers at similar relative contributions, as reflected by the two closely spaced C = C stretchings of the retinal chain at 1540 and 1550 cm<sup>-1</sup> (Fig. 2A). Both chromophores are attached to the protein via protonated Schiff bases that give rise to two C = N stretching modes at 1633 and 1652 cm<sup>-1</sup>. The significant frequency difference between these two bands, which shift down to 1621 cm<sup>-1</sup> upon H/D exchange (Fig. 2, *inset*), can at least partly be related to different hydrogen bonding or electrostatic interactions with the counter ion (21). For the Rh-UV state, however, there is no indication for structural heterogeneity of the chromophore (Fig. 2B). The C = C stretching mode at 1566 cm<sup>-1</sup> displays a symmetric bandshape, and there is only a

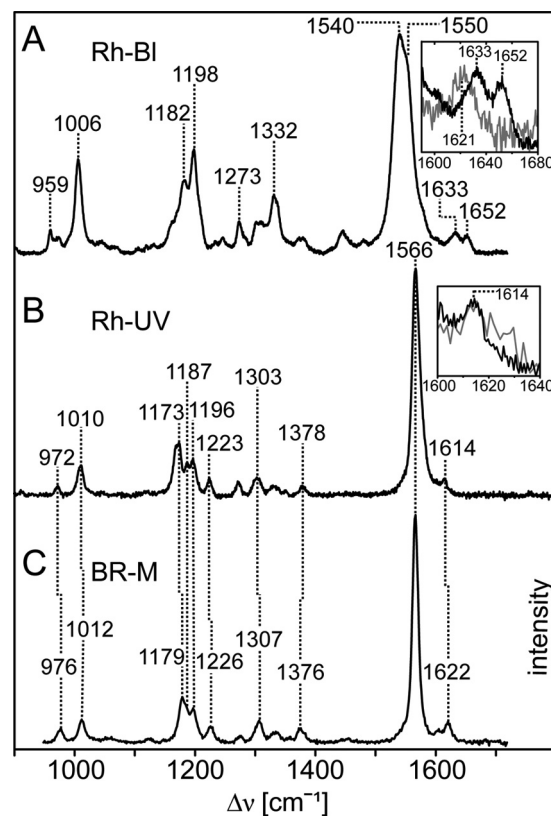


**FIGURE 2. Resonance Raman spectra of the two Rh isoforms.** *A*, spectrum of Rh-Bl, obtained with 514-nm excitation and UV LED irradiation. *B*, spectrum of Rh-UV, obtained with 413-nm excitation and blue LED irradiation. *C*, spectrum of the bacteriorhodopsin M412 state measured in a pump (514-nm) probe (413-nm) time-resolved resonance Raman experiment. Raman bands of the buffer have been subtracted. *C* = N stretching modes in H<sub>2</sub>O (black) and D<sub>2</sub>O (gray) are compared in the *inset*.

single band in the C = N stretching region at 1614 cm<sup>-1</sup>. The relatively low frequency of this band and the lack of isotopic shifts upon H/D exchange indicate a deprotonated Schiff base (Fig. 2, *inset*). In fact, comparison with the resonance Raman spectrum of the M410 state of bacteriorhodopsin comprising a deprotonated 13-*cis* retinal Schiff base demonstrates extensive similarities, with only small frequency differences for the conjugate bands (Fig. 2, *B* and *C*).

**Transition Dynamics between Rh-UV and Rh-Bl**—Next, these were analyzed by flash photolysis on the microsecond to second time scale. The protein was accumulated in the UV state by a 1-s 480-nm LED light pulse and subsequently stimulated with a UV laser flash. Spectra were recorded at different times after the flash. Very little change was seen between 1 μs and 500 μs before the Rh-Bl appeared, with a rise time of  $\tau = 2.3$  ms (Fig. 3, *A* and *B*). No significant absorption change was seen during the conversion from Rh-UV to Rh-Bl, leading to the question of how the light energy was stored for such a long time before protonation of the retinal Schiff base occurred during the appearance of Rh-Bl. In contrary, the phototransformation from Rh-Bl back to Rh-UV resembles the photoinduced processes of known retinal proteins. Immediately after a blue laser flash, an early photointermediate, P560, appeared, which relaxed with a  $\tau$  of 3.5 ms to a second species (P570) with a further red-shifted absorption. The latter disappeared with  $\tau$  of

## A UV-sensitive Algal Rhodopsin

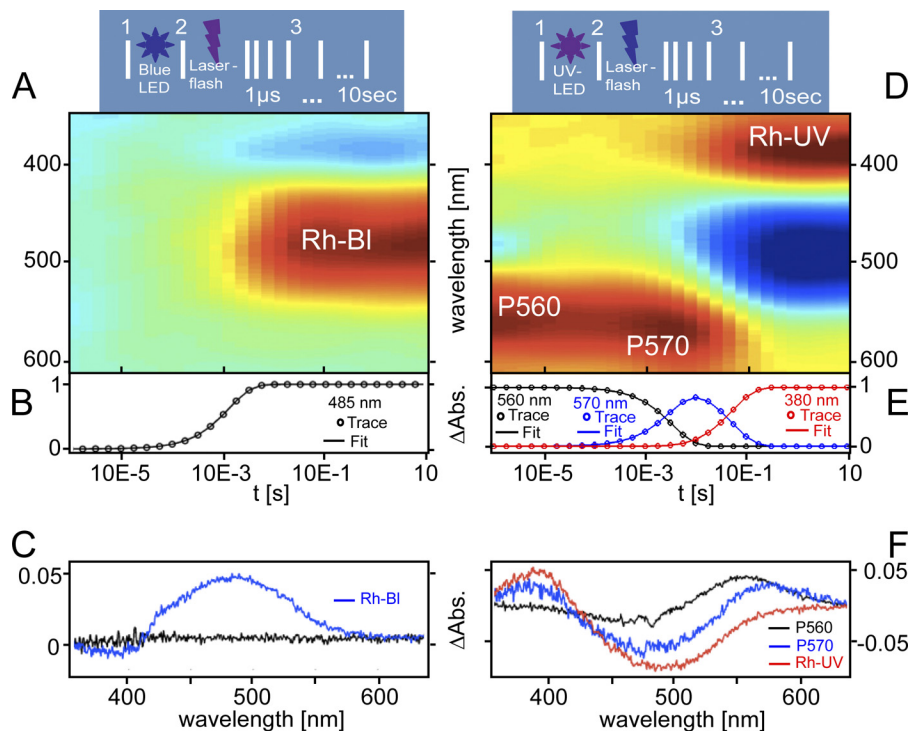


**FIGURE 3. Dynamics of the Rh-UV/Rh-Bl transitions.** *A* and *D*, illumination protocol and three-dimensional reconstructions of time-resolved absorbance changes of Rh-UV (*A*) and Rh-Bl (*D*) at pH 7 after 10-ns laser flashes of 380 (*A*) and 480 nm (*D*). Samples were illuminated for 2 s with a 480- (*A*) or 380-nm (*D*) LED prior to flash application. *B* and *E*, time course of individual components as they appear from singular value decomposition analysis. *C* and *F*, typical different spectra at selected times after flash.

54 ms upon the formation of the Rh-UV state (Fig. 3, *D* and *E*); the difference spectra of the intermediates are shown in Fig. 3*F*.

To decipher the early processes of the photoreactions, especially those of Rh-UV, we investigated the reactions of Rh-UV. Absorbance changes between 360 and 670 nm were recorded after excitation at 350 nm with a pulse width of about 80 fs at delay times of up to 3.5 ns. Background illumination of 450 nm was applied to keep the gross amount of Rh in the UV state. The time-resolved data were globally analyzed in terms of a sequential scheme of interconverting evolution-associated difference spectra (EADS) with increasing lifetimes (1->2->3->...). The first EADS (Fig. 4*A*, black) shows ground-state bleaching (GSB) near 380 nm and a broad excited-state absorption (ESA) that features two bands at ~480 nm and 580 nm and can be assigned to the initially prepared excited state. This EADS evolves in 365 fs into the red EADS, which shows a small blue shift of the ESA to ~470 nm, a slight loss between 500 and 670 nm, and a general narrowing of the absorbance features. The red EADS evolves within 5 ps into the green EADS, which is spectrally similar (Fig. 4*A*, green dashed spectrum) and shows an amplitude loss of approximately 50%. This EADS then decays within 60 ps into the nondecaying EADS (blue line in Fig. 4*A*), which shows an amplitude decrease to almost zero, leaving only a very small bleach at around 425 nm and an even smaller induced absorption near 450 nm. The kinetics of photoproduct formation are illustrated nicely by the absorbance change at 402 nm, which features both the large initial GSB and the small final product bleach (Fig. 4*B*).

We interpret the spectral evolution as follows. (i) Upon preparation of the excited state in the Franck-Condon region, struc-

tural and/or vibrational relaxation takes place in 365 fs, resulting in narrowing and blue-shifting of the ESA. (ii) The relaxed excited state decays biexponentially with time constants of 5 and 60 ps, most likely due to the conformational heterogeneity of the protein. (iii) The final spectrum has a very small amplitude, which implies that the primary photoproduct has absorption characteristics that are very similar to that of the Rh-UV parent state. We propose that isomerization of the RSB takes place with time constants of 5 and 60 ps, but that due to a lack of chromophore-protein interactions, absorption changes after the isomerization of deprotonated RSB are very low. This interpretation is in line with the μs to ms flash photolysis experiments of Fig. 3, which show a spectrally silent deprotonated species before protonation occurs in 2.3 ms. The excited state lifetimes of 5 and 60 ps are unusually long for a rhodopsin (22, 23). A study on unprotonated Schiff base model compounds showed that decreasing the polarity of the environment strongly increases the excited state lifetime (24). Thus, the long lifetime of the Rh-UV S1 state is fully consistent with an unusually unpolar retinal binding pocket. Next, femtosecond transient absorption spectroscopy was performed on Rh-Bl, with excitation at 500 nm and constant background illumination at 380 nm, to recover Rh-Bl. Global analysis indicated that four kinetic components are required for a satisfactory fit; the corresponding EADS are shown in Fig. 4*C*. The first EADS (black) is attributed to the initially prepared excited state of Rh-Bl, featuring a GSB at 480 nm and the ESA at 570 nm. This EADS evolves into the red EADS in 643 fs, which shows a similar GSB at reduced amplitude and a blue-shifted, narrowed ESA near 560 nm, indicative of structural and/or vibrational relaxation in

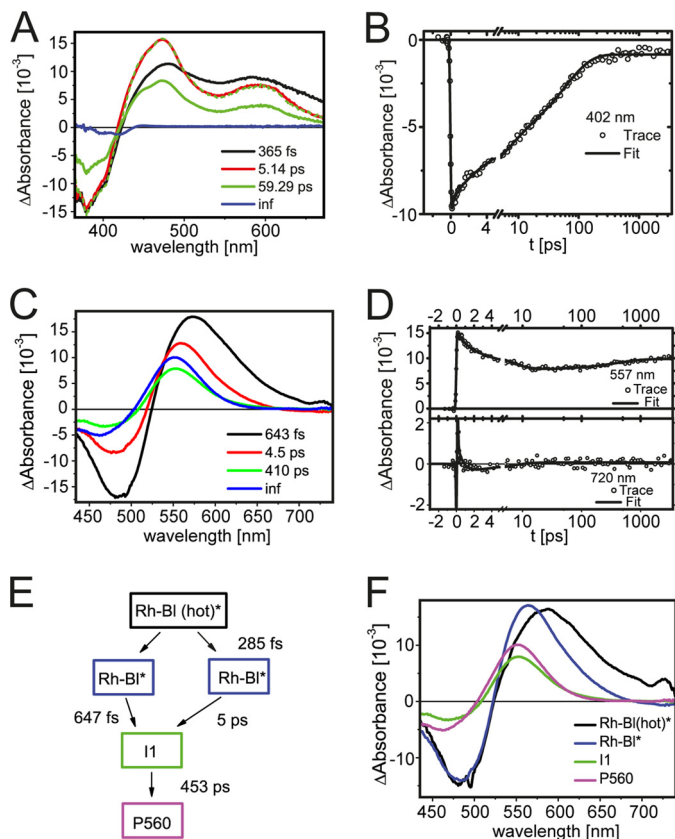


**FIGURE 4. Ultrafast dynamics of Rh-UV and Rh-Bl.** *A*, spectral evolution of Rh-UV after excitation at 350 nm is illustrated by sequentially interconverting EADS with their corresponding lifetimes. *B*, kinetic trace at 402 nm and its corresponding fit show the evolution of the GSB of Rh-UV into the final photoproduct. The green dashed spectrum in *A* represents the green EADS scaled by a factor of 1.9 and shows the almost identical spectral signature of the red and green EADS. *C*, spectral evolution of Rh-Bl is displayed after excitation according to a model with sequentially interconverting EADS and their corresponding lifetimes. *D*, absorbance change at 557 nm after 500 nm excitation illustrates the spectral evolution of Rh-Bl into the P560 intermediate. At early times the absorption corresponds to the decay of excited state absorption, whereas at later times the absorption increases due to P560 formation. The kinetic trace at 720 nm (*D*) shows a fast decay of excited state absorption into a small negative feature corresponding to stimulated emission. *E* and *F*, spectral evolution of Rh-Bl after 500-nm excitation was analyzed using a branched model (*E*) with the corresponding species-associated difference spectra (*F*).

the excited state. Additionally, a negative signal is observed around 720 nm, attributed to stimulated emission. As a result of extensive overlap with ESA, the stimulated emission signal is small. The next EADS (green) is formed in 4.5 ps. It features an overall loss in amplitude and a further blue shift of both the GSB (475 nm) and induced absorbance (550 nm). The final, nondecaying EADS is formed in 410 ps and shows a further blue shift of the GSB (460 nm) and an overall increase in intensity. The final EADS shows remarkable similarity to the difference spectrum obtained in the flash photolysis experiment after 1  $\mu$ s (P560). A simple target model (Fig. 4E) was applied to the transient data set, which, in contrast to the sequential model described above, allows the disentanglement of branched reactions and ideally produces the true, so-called species-associated difference spectra. We included relaxation of the excited state, with subsequent biexponential decay to an intermediate (I1), and a final, nondecaying species, which is identical to the P560.

intermediate from flash photolysis. Similar to previous investigations on channelrhodopsin-2 from *C. reinhardtii* (25), we observe species-associated difference spectra (Fig. 4F) characteristic of vibrational and/or structural relaxation of the excited state in <300 fs, followed by a biexponential decay with 0.6 and 5 ps into I1. The excited state lifetimes are visible in the decay of stimulated emission at 720 nm (Fig. 4D) within the first 20 ps after the relaxation of the primary excited state. The I1 intermediate shows an overall blue shift of the difference spectrum compared with the excited state, along with a significant loss in signal. This difference spectrum represents a red shift of the absorbance of Rh-Bl, similar to that observed for J and K intermediates in bacteriorhodopsin (BR) (23). The final P560 intermediate is formed from I1 within 400 ps along with a blue shift, an increase in negative contributions, and an increase but no spectral shift in the induced absorption. This behavior is also clearly illustrated by the absorbance change at 527 nm (Fig. 4D), which shows excited state absorption decaying within the first 20 ps and a slow increase at later delay times.

## DISCUSSION

The first spectroscopically characterized UV-rhodopsin belongs to a yet-uncharacterized class of HKRs (supplemental Fig. 2). The localization of HKR1 within the eyespot of *C. reinhardtii* originally surprised us because phototaxis was thought to be mediated exclusively by the channelrhodopsins ChR1 and ChR2 (26, 27), and control of photobehavior has been considered the major if not exclusive role of the eye.

However, because the proposed photoreceptor Chlamyopsin-2 (Cop2), which is involved in the assembling of photosystem-1 (28), is also localized in the eye, it appears to be that algal eyes are more general sensory organelles. Furthermore, the fact that the dark-adapted Rh of HKR1 absorbs in the UV range is surprising because, to our knowledge, no specific UV response has ever been described for *C. reinhardtii*, suggesting that HKR1 mediates more general UV avoidance reactions or simply UV stress responses that modify sensory processes in the presence of UVA light. We have so far been unable to functionally reconstitute the complete HKR1 in *E. coli* or *Xenopus* oocytes as we have done previously for the small photoactivated cyclase bPAC (13); therefore, we do not know whether HKR1 is a guanylyl cyclase or an adenylyl cyclase. cAMP has been suggested as an abiotic stress metabolite in *C. reinhardtii* whereas the role of cGMP is unknown. Intraflagellar cAMP increases upon sexual agglutination to reduce flagellar motility after the mating partners come in contact (29). A regulatory role of cAMP within the eyespot organelle is conceivable. UVA-sensitive microbial rhodopsins have not been described so far but are now expected to be present in many algae. Functions for this “new” rhodopsin subfamily await further elucidation. *C. reinhardtii* additionally contains a UVB receptor, whose homolog, UVR8, has been recently characterized in *Arabidopsis* (30). This protein uses tryptophan side chains arranged in an excitationally coupled cluster at the dimer interface as the sole intrinsic receptor pigment. Excitation with 280 nm leads to monomerization of the protein and binding to COP1 (CONSTITUTIVELY PHOTOMORPHOGENIC 1), resulting in a general photoprotection response.

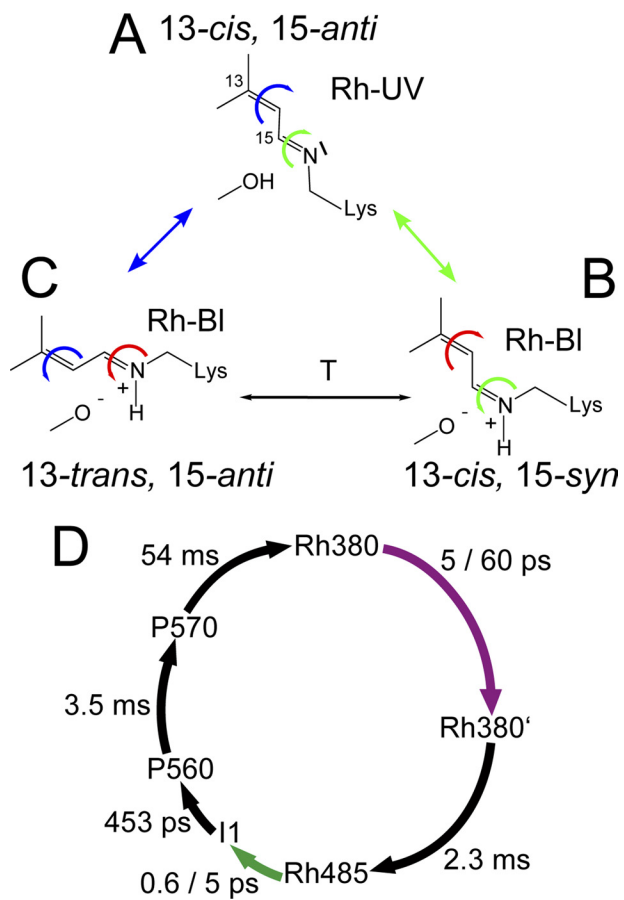


FIGURE 5. A–C, schematic representation of the  $13 = 14$  and  $15 = N$  conformers of the retinal Schiff base. Possible isomerizations are indicated by colored arrows. We conclude that the conformation of the Rh-UV state is 13-cis,15-anti (A), whereas Rh-Bl represents an equilibrium of 13-cis,15-anti (B) and 13-trans,15-anti (all-trans) (C). The two Rh-Bl conformers thermally equilibrate by double isomerizations (red+blue or red+green). D, proposed photocycle summarizing interconversion of the light-induced reaction intermediates as observed after 380-nm excitation (purple arrow) and 500-nm excitation (green arrow) in ultrafast and flash photolysis spectroscopic experiments.

The large photochromic shifts as found for HKR1 and the great stability of Rh-UV are unprecedented findings for a microbial rhodopsin. Such photochromism is commonly found in fly rhodopsins or in retinochromes (31). Small fully reversible photochromic shifts have been reported for *Anabaena* sensory rhodopsin where orange illumination of the dark state ( $\lambda_{\text{max}} = 549$  nm) photoisomerizes all-trans retinal into 13-cis light-adapted state ( $\lambda_{\text{max}} = 537$  nm) that is stable for a few hundred minutes (32). Phototactic signaling in archaea by sensory rhodopsin I is mediated via a bimodal photochemical switching between the dark state absorbing at 590 and the signaling state with deprotonated chromophore absorbing at 370 nm (P370) (33). However, the thermal life time for the signaling state is a half-second and not hours as in the case of HKR1. From the molecular aspect, it is very interesting to know why the chromophore is deprotonated in its most stable dark state. Because the resonance Raman spectra are sensitive to both 13-cis/trans and 15-syn/anti isomerization (Fig. 5), the excellent agreement between the Raman spectra of Rh-UV and the BR-M410 photocycle intermediate points to a 13-cis configuration of the RSB with an anti conformation of the C = N bond (13-cis,15-anti)

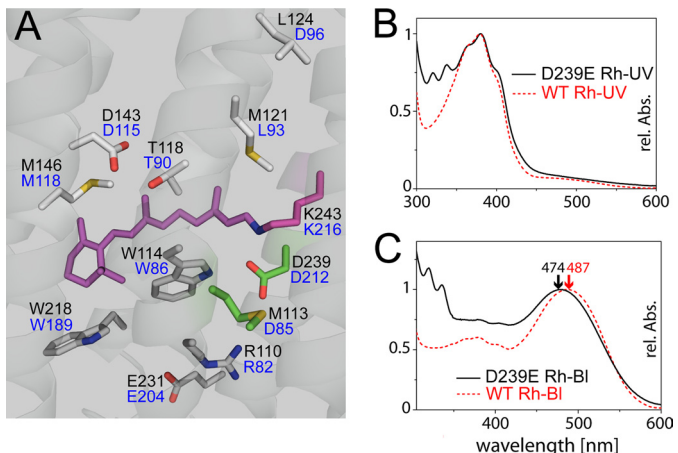


FIGURE 6. Active site. A, homology model of HKR1 based on BR. The model shows a seven-transmembrane structure and a lysine to bind the chromophore. The retinal and conserved residues in the retinal binding pocket (HKR1, black; BR, blue), are highlighted in color. B and C, normalized absorbance spectra of the HKR mutant D239E (solid lines) compared with wild-type (WT) HKR1. The WT and D239E Rh-UV forms have an absorbance maximum at 380 nm (B). The aggregation tendency of the purified mutant causes increased scattering. The absorbance maximum of D239E-Rh-Bl shows a 13-nm shift to lower wavelengths and more scattering in the UVA-region (C).

(34, 35). There are no indications for contributions by an all-trans chromophore because the respective characteristic marker bands, such as a distinct band at  $1153\text{ cm}^{-1}$ , are not detectable in the Raman spectrum (34). Homology modeling with structures of other microbial rhodopsins as bacteriorhodopsin, halorhodopsin, SRII, and channelrhodopsin C1C2 (Fig. 6), for which three-dimensional structures are available (36–38), led to the assumption that in a 13-cis,15-anti configuration (Fig. 5A) the free electron pair of the Schiff base nitrogen is facing away from the *bona fide* counterion Asp-239. This configuration makes protonation of the nitrogen highly unfavorable as in the BR-M state, where the  $pK_a$  of the Schiff base is 7 units lower compared with the dark state. In contrast, for Rh-Bl we suggest that the electron pair of the Schiff base nitrogen is facing toward Asp-239, thereby stabilizing the protonated state. In this case, two states, 13-cis,15-syn and 13-trans,15-anti, could accomplish this condition (Fig. 5, B and C). Consistent with the Raman data, both such states could exist in slow thermal equilibrium in the Rh-Bl state. This is not unlikely because exactly these two states do coexist in dark-adapted BR, as shown most clearly by nuclear magnetic resonance (NMR) spectroscopy (36). We challenged the claim that Asp-239 is the counterion of the retinal Schiff base by substituting Asp-239 by Glu and Asn. D239N did not form a chromophore whereas D239E-Rh-Bl did (Fig. 6B), and the absorption of the blue state was hypsochromically shifted by 13 nm (Fig. 6C). Photoconversion from Rh-UV to Rh-Bl involves a branched reaction pathway leading to two chromophore isomers with protonated Schiff bases, attributed to an all-trans and 13-cis configuration, respectively. A possible explanation may be that photoexcitation of Rh-UV leads to an electronically excited state that allows for both a rotation around the C(13) = C(14) double bond (Fig. 5, blue arrow) and for an anti/syn isomerization of the C(15) = N Schiff base in principle (Fig. 5, green arrow). This dual option of molecular events may be a tribute to the unusually long life-

time of the electronically excited state of  $\sim$ 60 ps in case of Rh-UV. A sole *anti/syn* isomerization around the C(15) = N bond has been described for the photochemical transition from the Meta-II to Meta-III states of rod bovine rhodopsin (39). In contrast to the unusual photochemistry of Rh-UV, Rh-Bl shows typical rhodopsin photochemistry as observed in BR and channelrhodopsin. Therefore, it might be conceivable that the two excited state deactivation pathways originate from the two proposed isomers, which are not necessarily both productive for the Rh-UV state. Due to the high stability of the Rh-UV state and thermal equilibrium between both proposed Rh-Bl retinal conformations, it is nevertheless possible to create Rh-UV quantitatively by continuous illumination. In conclusion, the rhodopsin part of HKR1 can switch between two isoforms Rh-UV and Rh-Bl that are both thermally stable in darkness but are efficiently interconverted by UV and blue light. Rh-UV is unusual in the sense that the excited state lifetime is exceptionally long and the early photoproducts are hardly seen as changes in the visible spectrum. The underlying processes await further elucidation, for example by infrared studies on an ultrafast time scale.

**Acknowledgments**—We thank Christina Mrosek and Margrit Michalsky for excellent technical assistance and Eglof Ritter and Patrick Piwowarski for support with the HPLC.

## REFERENCES

1. Kleinschmidt, J., and Harosi, F. I. (1992) Anion sensitivity spectral tuning of cone visual pigments *in situ*. *Proc. Natl. Acad. Sci. U.S.A.* **89**, 9181–9185
2. Imai, H., Hirano, T., Terakita, A., Shichida, Y., Muthyalu, R. S., Chen, R. L., Colmenares, L. U., and Liu, R. S. (1999) Probing for the threshold energy for visual transduction: red-shifted visual pigment analogs from 3-methoxy-3-dehydroretinal and related compounds. *Photochem. Photobiol.* **70**, 111–115
3. Luo, D. G., Yue, W. W., Ala-Laurila, P., and Yau, K. W. (2011) Activation of visual pigments by light and heat. *Science* **332**, 1307–1312
4. Kusnetzow, A. K., Dukkipati, A., Babu, K. R., Ramos, L., Knox, B. E., and Birge, R. R. (2004) Vertebrate ultraviolet visual pigments: protonation of the retinylidene Schiff base and a counterion switch during photoactivation. *Proc. Natl. Acad. Sci. U.S.A.* **101**, 941–946
5. Tarttelin, E. E., Bellingham, J., Hankins, M. W., Foster, R. G., and Lucas, R. J. (2003) Neuropsin (Opn5): a novel opsin identified in mammalian neural tissue. *FEBS Lett.* **554**, 410–416
6. Gao, R., and Stock, A. M. (2009) Biological insights from structures of two-component proteins. *Annu. Rev. Microbiol.* **63**, 133–154
7. Zhang, F., Vierock, J., Yizhar, O., Fenno, L. E., Tsunoda, S., Kianianmomeni, A., Prigge, M., Berndt, A., Cushman, J., Polle, J., Magnuson, J., Hegemann, P., and Deisseroth, K. (2011) The microbial opsin family of optogenetic tools. *Cell* **147**, 1446–1457
8. Kateriya, S., Nagel, G., Bamberg, E., and Hegemann, P. (2004) “Vision” in single-celled algae. *News Physiol. Sci.* **19**, 133–137
9. Troein, C., Corellou, F., Dixon, L. E., van Ooijen, G., O’Neill, J. S., Bouget, F. Y., and Millar, A. J. (2011) Multiple light inputs to a simple clock circuit allow complex biological rhythms. *Plant J.* **66**, 375–385
10. Kolaskar, A. S., and Tongaonkar, P. C. (1990) A semiempirical method for prediction of antigenic determinants on protein antigens. *FEBS Lett.* **276**, 172–174
11. Bamann, C., Kirsch, T., Nagel, G., and Bamberg, E. (2008) Spectral characteristics of the photocycle of channelrhodopsin-2 and its implication for channel function. *J. Mol. Biol.* **375**, 686–694
12. Bruun, S., Naumann, H., Kuhlmann, U., Schulz, C., Stehfest, K., Hegemann, P., and Hildebrandt, P. (2011) The chromophore structure of the long-lived intermediate of the C128T channelrhodopsin-2 variant. *FEBS Lett.* **585**, 3998–4001
13. Stierl, M., Stumpf, P., Udwari, D., Gueta, R., Hagedorn, R., Losi, A., Gärtner, W., Petereit, L., Efetova, M., Schwarzel, M., Oertner, T. G., Nagel, G., and Hegemann, P. (2011) Light modulation of cellular cAMP by a small bacterial photoactivated adenylyl cyclase, bPAC, of the soil bacterium *Beggiatoa*. *J. Biol. Chem.* **286**, 1181–1188
14. Stehfest, K., Ritter, E., Berndt, A., Bartl, F., and Hegemann, P. (2010) The branched photocycle of the slow-cycling channelrhodopsin-2 mutant C128T. *J. Mol. Biol.* **398**, 690–702
15. Berera, R., van Grondelle, R., and Kennis, J. T. (2009) Ultrafast transient absorption spectroscopy: principles and application to photosynthetic systems. *Photosynth. Res.* **101**, 105–118
16. Mathes, T., Zhu, J. Y., van Stokkum, I. H. M., Groot, M. L., Hegemann, P., and Kennis, J. T. M. (2012) Hydrogen bond switching among flavin and amino acids determines the nature of proton-coupled electron transfer in BLUF photoreceptors. *J. Phys. Chem. Lett.* **3**, 203–208
17. Snellenburg, J. J., Laptenok, S. P., Seger, R., Mullen, K. M., and van Stokkum, I. H. M. (2012) Glotaran: a Java-based graphical user interface for the R-package TIMP. *J. Statistical Software* **49**, 1–22
18. Ly, H. K., Wisitruangsakul, N., Sezer, M., Feng, J. J., Kranich, A., Weidinger, I. M., Zebger, I., Murgida, D. H., and Hildebrandt, P. (2011) Electric field effects on the interfacial electron transfer and protein dynamics of cytochrome c. *J. Electroanal. Chem.* **660**, 367–376
19. Naumann, H., Murgida, D. H., Engelhard, M., Klare, J. P., and Hildebrandt, P. (2006) Time-resolved resonance Raman spectroscopy of sensory rhodopsin II in the micro- and millisecond time range using gated cw excitation. *J. Raman Spectrosc.* **37**, 436–441
20. Landers, G. M., and Olson, J. A. (1988) Rapid, simultaneous determination of isomers of retinal, retinal oxime and retinol by high-performance liquid chromatography. *J. Chromatogr.* **438**, 383–392
21. Gerscher, S., Mylrajan, M., Hildebrandt, P., Baron, M. H., Müller, R., and Engelhard, M. (1997) Chromophore-anion interactions in halorhodopsin from *Natronobacterium pharaonis* probed by time-resolved resonance Raman spectroscopy. *Biochemistry* **36**, 11012–11020
22. Lutz, I., Sieg, A., Wegener, A. A., Engelhard, M., Boche, I., Otsuka, M., Oesterhelt, D., Wachtveitl, J., and Zinth, W. (2001) Primary reactions of sensory rhodopsins. *Proc. Natl. Acad. Sci. U.S.A.* **98**, 962–967
23. Polland, H. J., Franz, M. A., Zinth, W., Kaiser, W., Kölling, E., and Oesterhelt, D. (1986) Early picosecond events in the photocycle of Bacteriorhodopsin. *Biophys. J.* **49**, 651–662
24. Bachilo, S. M., and Gillbro, T. (1999) Fluorescence of retinal Schiff base in alcohols. *J. Phys. Chem. A* **103**, 2481–2488
25. Verhoeven, M. K., Bamann, C., Blöcher, R., Förster, U., Bamberg, E., and Wachtveitl, J. (2010) The photocycle of channelrhodopsin-2: ultrafast reaction dynamics and subsequent reaction steps. *ChemPhysChem* **11**, 3113–3122
26. Berthold, P., Tsunoda, S. P., Ernst, O. P., Mages, W., Gradmann, D., and Hegemann, P. (2008) Channelrhodopsin-1 initiates phototaxis and photophobic responses in *Chlamydomonas* by immediate light-induced depolarization. *Plant Cell* **20**, 1665–1677
27. Sineschekov, O. A., Jung, K. H., and Spudich, J. L. (2002) Two rhodopsins mediate phototaxis to low- and high-intensity light in *Chlamydomonas reinhardtii*. *Proc. Natl. Acad. Sci. U.S.A.* **99**, 8689–8694
28. Ozawa, S., Nield, J., Terao, A., Stauber, E. J., Hippler, M., Koike, H., Rochaix, J. D., and Takahashi, Y. (2009) Biochemical and structural studies of the large Ycf4-photosystem I assembly complex of the green alga *Chlamydomonas reinhardtii*. *Plant Cell* **21**, 2424–2442
29. Saito, T., Small, L., and Goodenough, U. W. (1993) Activation of adenylyl cyclase in *Chlamydomonas reinhardtii* by adhesion and by heat. *J. Cell Biol.* **122**, 137–147
30. Christie, J. M., Arvai, A. S., Baxter, K. J., Heilmann, M., Pratt, A. J., O’Hara, A., Kelly, S. M., Hothorn, M., Smith, B. O., Hitomi, K., Jenkins, G. I., and Getzoff, E. D. (2012) Plant UVR8 photoreceptor senses UV-B by tryptophan-mediated disruption of cross-dimer salt bridges. *Science* **335**, 1492–1496
31. Furutani, Y., Terakita, A., Shichida, Y., and Kandori, H. (2005) FTIR studies of the photoactivation processes in squid retinochrome. *Biochemistry* **44**, 7988–7997

## A UV-sensitive Algal Rhodopsin

32. Vogeley, L., Sineshchekov, O. A., Trivedi, V. D., Sasaki, J., Spudich, J. L., and Luecke, H. (2004) *Anabaena* sensory rhodopsin: a photochromic color 0 sensor at 2.0 angstrom. *Science* **306**, 1390–1393
33. Spudich, J. L., and Bogomolni, R. A. (1984) Mechanism of color discrimination by a bacterial sensory rhodopsin. *Nature* **312**, 509–513
34. Curry, B., Palings, I., Broek, A. D., Pardon, J. A., Lugtenburg, J., and Mathies, R. (1985) Vibrational analysis of the retinal isomers. *Adv. Infrared Raman Spectrosc.* **12**, 115–178
35. Fodor, S. P., Ames, J. B., Gebhard, R., van den Berg, E. M. M., Stoeckenius, W., Lugtenburg, J., and Mathies, R. A. (1988) Chromophore structure in bacteriorhodopsins-N intermediate: implications for the proton-pumping mechanism. *Biochemistry* **27**, 7097–7101
36. Schobert, B., Lanyi, J. K., Spudich, E. N., and Spudich, J. L. (2001) Crystal structure of sensory rhodopsin II at 2.4 angstroms: insights into color tuning and transducer interaction. *Science* **293**, 1499–1503
37. Kolbe, M., Besir, H., Essen, L. O., and Oesterhelt, D. (2000) Structure of the light-driven chloride pump halorhodopsin at 1.8 angstrom resolution. *Science* **288**, 1390–1396
38. Kato, H. E., Zhang, F., Yizhar, O., Ramakrishnan, C., Nishizawa, T., Hirata, K., Ito, J., Aita, Y., Tsukazaki, T., Hayashi, S., Hegemann, P., Maturana, A. D., Ishitani, R., Deisseroth, K., and Nureki, O. (2012) Crystal structure of the channelrhodopsin light-gated cation channel. *Nature* **482**, 369–374
39. Ritter, E., Zimmermann, K., Heck, M., Hofmann, K. P., and Bartl, F. J. (2004) Transition of rhodopsin into the active metarhodopsin II state opens a new light-induced pathway linked to Schiff base isomerization. *J. Biol. Chem.* **279**, 48102–48111

**Molecular Biophysics:  
A Photochromic Histidine Kinase  
Rhodopsin (HKR1) That Is Bimodally  
Switched by Ultraviolet and Blue Light**

Meike Luck, Tilo Mathes, Sara Bruun, Roman Fudim, Rolf Hagedorn, Tra My Tran Nguyen, Suneel Kateriya, John T. M. Kennis, Peter Hildebrandt and Peter Hegemann

*J. Biol. Chem.* 2012, 287:40083-40090.

doi: 10.1074/jbc.M112.401604 originally published online October 1, 2012

MOLECULAR  
BIOPHYSICS

PLANT BIOLOGY

Access the most updated version of this article at doi: [10.1074/jbc.M112.401604](https://doi.org/10.1074/jbc.M112.401604)

Find articles, minireviews, Reflections and Classics on similar topics on the [JBC Affinity Sites](#).

Alerts:

- [When this article is cited](#)
- [When a correction for this article is posted](#)

[Click here](#) to choose from all of JBC's e-mail alerts

Supplemental material:

<http://www.jbc.org/content/suppl/2012/10/01/M112.401604.DC1.html>

This article cites 39 references, 15 of which can be accessed free at  
<http://www.jbc.org/content/287/47/40083.full.html#ref-list-1>